# Supplementary Material:

# Flexibility and charge asymmetry in the activation loop of Src tyrosine kinases

Nilesh K. Banavali and Benoît Roux

Submitted to *Proteins: Structure, Function, and Bioinformatics* , March 6, 2008.

# Convergence of the free energy profiles describing activation loop flexibility

As mentioned in the methods section, 10 different restrained simulations (5 forward f1-f5, 5 backward b1-b5) were carried out to model the transitions of the hydrophilic part of the activation loop. The starting and ending point reference states were the crystal structure of the Y416-buried conformation of the loop (PDB ID: 1QCF) and the artificially modeled Y416-exposed state where only the hydrophilic part of the activation loop (residues 412:424) is in its active state conformation, while the rest of the kinase (including the hydrophobic part of the activation loop: residues 403-411) is still in its inactive state. These reference states provide an ideal span of the $\Delta D_{\mathrm{RMSD}}$ parameter since the structures that they evolve to upon equilibration for a few ns lie within the span defined by them. Monitoring the initial behavior of all simulations with respect to their calculated free energy profile along the $\Delta D_{\mathrm{RMSD}}$ parameter showed that the 5 forward simulations mostly resembled each other and the 5 backward simulations mostly resembled each other. When classified together, however, the forward simulation class and the backward simulation class differed significantly from each other (data not shown).

Since these differences were most likely the result of hysteresis due to lack of sampling, specific simulations that either showed traits of appearance of minima identified in the other class (f3, f4, and b2) or did not show such traits at all (f5 and b5) were chosen to be extended further up to at least 1.4 ns per window. Here, the forward simulations (f3, f4, and f5) varied from the backward simulations (b2 and b5) in that further sampling showed a significant change in calculated free energy profiles. A minima appeared near the $\Delta D_{\mathrm{RMSD}}$ value of 0 in these forward simulations (which is the lowest energy minima for all backward simulations) and grew progressively lower in energy, so much so that its relative energy started to become lower than the minima close to the Y416-buried starting structure. This behavior was observed in all three forward simulations that were extended. The two backward simulations

that were extended, on the other hand, did not show such a pronounced appearance or reversal of minima. One forward (f5) and one backward simulation (b2) was extended further upto 2 ns per window. Since the forward simulation still did not seem to have converged, it was extended even further to 5 ns per window. The overall results for all 10 simulations are shown in Figure 1. Figure 2 shows the division of the sampling for the longest forward and backward simulations into 5 increments. The trends remain the same as those mentioned above and it is clear that the overall trend upon further sampling is stabilization of the broader minima near $\Delta D_{\mathrm{RMSD}}$ value of 0 and destabilization of the minima near $\Delta D_{\mathrm{RMSD}}$ value of -6. The overall free energy profiles reported are therefore expected to be accurate, and any errors are most likely in the underestimation of the instability of the Y416-buried conformations with respect to the Y416-exposed conformations that form the minima near $\Delta D_{\mathrm{RMSD}}$ value of 0.

# Sequence information showing charged residue asymmetry in Src kinase activation loops

The actual sequences used to infer the presence of charge asymmetry in hydrophilic sections of the activation loops of Src kinases are shown in Table 1. They are arranged according to the excess number of possible inter-segment charged interactions as compared to intra-segment charged interactions. The MD simulation analysis shows that inter-segment charged interactions can block Tyr416 from the environment, while intra-segment interactions do not. Such asymmetry provides a straightforward mechanism for facilitating release of the Tyr416 when the loop of another Src kinase molecule interacting with it is also asymmetric. Activation loop charged residues can simply exchange their intra-molecular interactions for inter-molecular interactions with complementary charged residues on the other kinase activation loop, thereby providing a path for access of Tyr416 to the active site of the other kinase molecule.

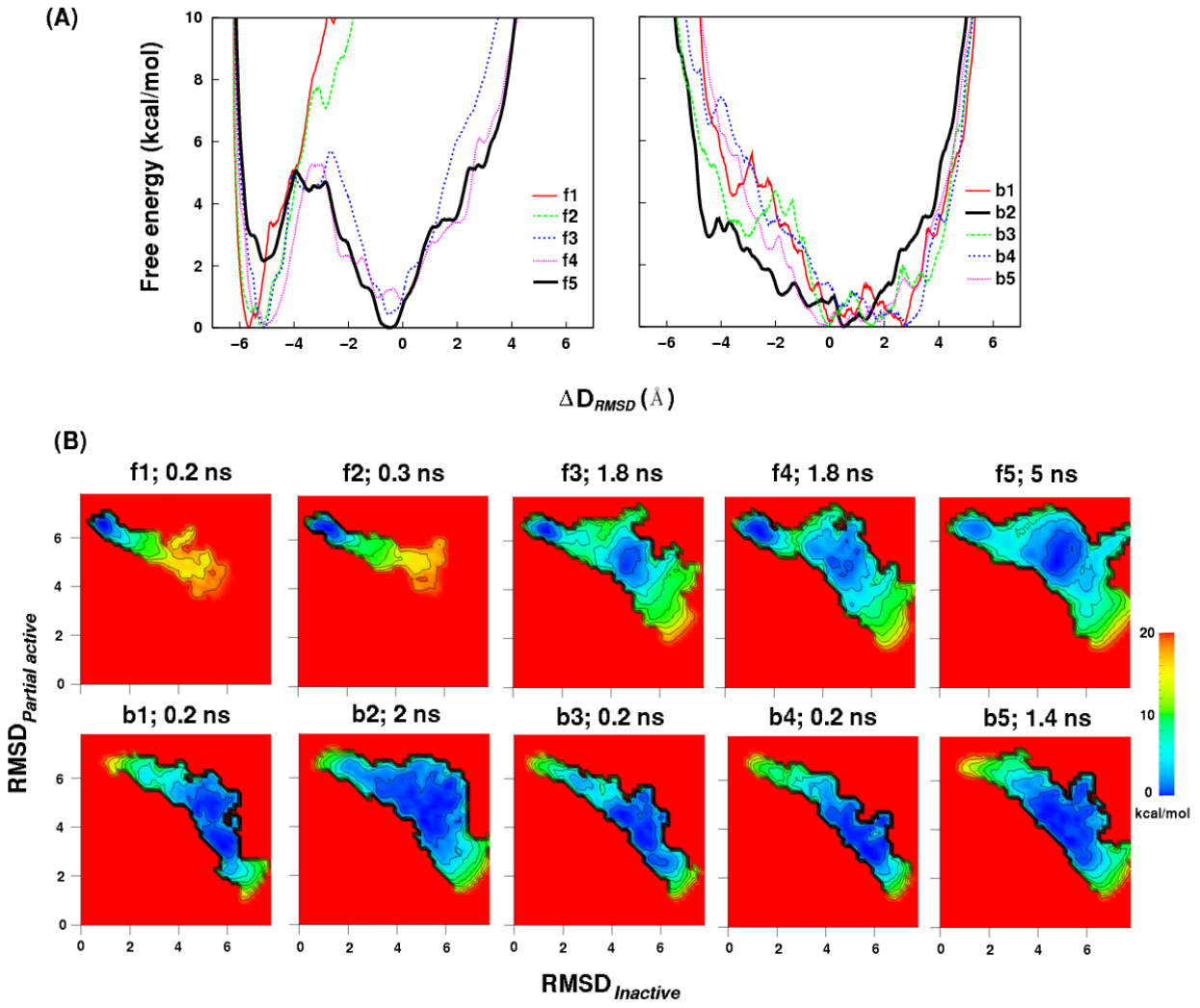


Figure 1: Free energy profiles describing conformational change in the hydrophilic part of the activation loop. (A) 1D free energy profiles along the $\Delta D_{\mathrm{RMSD}}$ parameter for 5 forward and 5 backward simulations, (B) 1D free energy profiles along individual RMSD values from 2 reference states for 5 forward and 5 backward simulations labeled with the amount of sampling per window for each simulation.

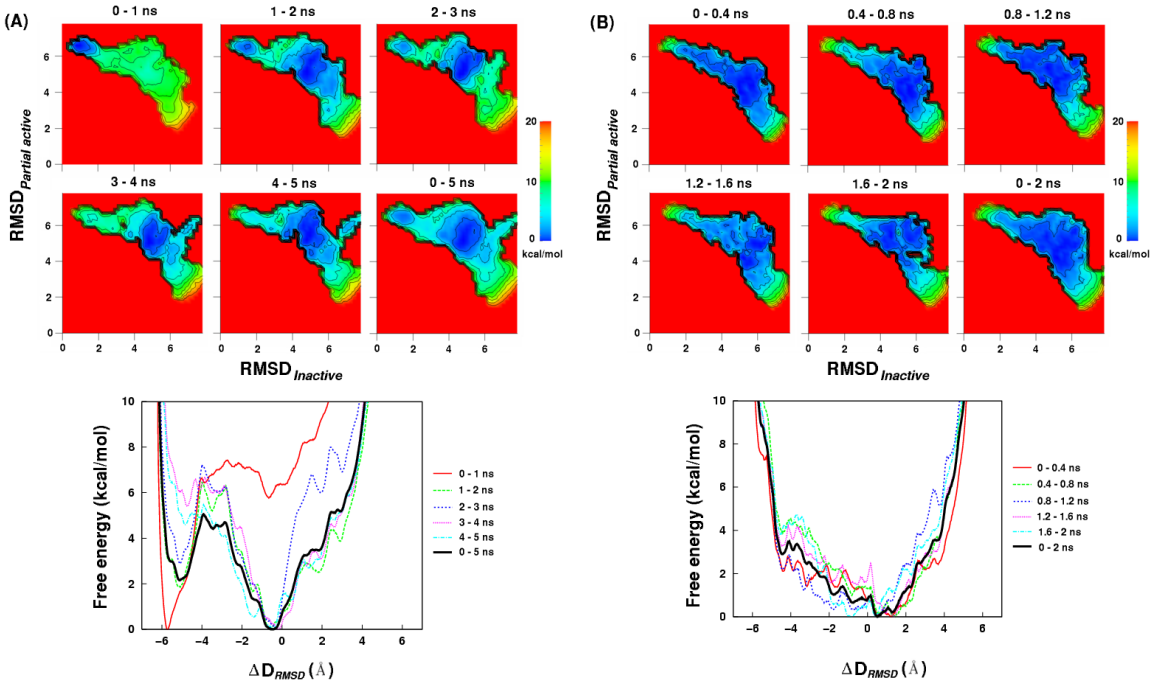


Figure 2: Convergence of free energy profiles describing conformational change in the hydrophilic part of the activation loop. (A) Longest forward simulation (f5) with 5 ns per window divided into five 1 ns increments, (B) Longest backward simulation (b2) with 2 ns per window divided into 5 0.4 ns increments.

Table 1: The 47 sequences used to infer the presence of charged residue asymmetry in activation loop segments of Src kinases with their Swiss-Prot primary accession numbers (ID). The sequences are sorted according to the difference between possible inter-segment and intra-segment charged residue interactions (Asymm), which signifies the ability of the two segments of the loop (residues 412-415 and residues 417-423) separated by Tyr416 to interact with each other to reduce accessibility of Tyr416 to the environment and increase plasticity of the hydrophilic part of the activation loop.

| Sequence | ID | Asymm | Sequence | ID | Asymm |
|---|---|---|---|---|---|
| DFGLARLIKDDEYNPCQGSKFPIKWTA | P09769 | 0 | DFGLARLIEDNEYTARQGAKFPIKWTA | P00525 | 6 |
| DFGLARII-DSEYTAQEGAKFPIKWTA | P16277 | 1 | DFGLARLIEDNEYTARQGAKFPIKWTA | P00526 | 6 |
| DFGLARII-DSEYTAQEGAKFPIKWTA | P51451 | 1 | DFGLARLIEDNEYTARQGAKFPIKWTA | P05480 | 6 |
| DFGLARLIKEDEYEARVGARFPIKWTA | Q9V9J3 | 2 | DFGLARLIEDNEYTARQGAKFPIKWTA | P06241 | 6 |
| DFGLARLIEDNEYNPQQGTKFPIKWTA | P14234 | 3 | DFGLARLIEDNEYTARQGAKFPIKWTA | P07947 | 6 |
| DFGLARIIEDNEYTAREGAKFPIKWTA | P08103 | 4 | DFGLARLIEDNEYTARQGAKFPIKWTA | P09324 | 6 |
| DFGLARIIEDNEYTAREGAKFPIKWTA | P50545 | 4 | DFGLARLIEDNEYTARQGAKFPIKWTA | P10936 | 6 |
| DFGLARIIEDNEYTAREGAKFPIKWTA | Q95M30 | 4 | DFGLARLIEDNEYTARQGAKFPIKWTA | P12931 | 6 |
| DFGLARLIEDNEYTAREGAKFPIKWTA | P06239 | 4 | DFGLARLIEDNEYTARQGAKFPIKWTA | P13115 | 6 |
| DFGLARLIEDNEYTAREGAKFPIKWTA | P06240 | 4 | DFGLARLIEDNEYTARQGAKFPIKWTA | P13116 | 6 |
| DFGLARLIEDNEYTAREGAKFPIKWTA | P42683 | 4 | DFGLARLIEDNEYTARQGAKFPIKWTA | P13406 | 6 |
| DFGLARLIEDNEYTAREGAKFPIKWTA | Q5PXS1 | 4 | DFGLARLIEDNEYTARQGAKFPIKWTA | P14084 | 6 |
| DFGLARLIEDNEYTAREGAKFPIKWTA | Q95KR7 | 4 | DFGLARLIEDNEYTARQGAKFPIKWTA | P14085 | 6 |
| DFGLARLIEDNEYTAREGAKFPIKWTA | Q95KR7 | 4 | DFGLARLIEDNEYTARQGAKFPIKWTA | P15054 | 6 |
| DFGLARVIEDNEYTAREGAKFPIKWTA | P07948 | 4 | DFGLARLIEDNEYTARQGAKFPIKWTA | P25020 | 6 |
| DFGLARVIEDNEYTAREGAKFPIKWTA | P07948 | 4 | DFGLARLIEDNEYTARQGAKFPIKWTA | P27446 | 6 |
| DFGLARVIEDNEYTAREGAKFPIKWTA | P08631 | 4 | DFGLARLIEDNEYTARQGAKFPIKWTA | P39688 | 6 |
| DFGLARVIEDNEYTAREGAKFPIKWTA | P25911 | 4 | DFGLARLIEDNEYTARQGAKFPIKWTA | P63185 | 6 |
| DFGLARVIEDNEYTAREGAKFPIKWTA | Q07014 | 4 | DFGLARLIEDNEYTARQGAKFPIKWTA | Q02977 | 6 |
| DFGLARLIEDNEYNPRQGAKFPIKWTA | P00544 | 6 | DFGLARLIEDNEYTARQGAKFPIKWTA | Q04736 | 6 |
| DFGLARLIEDNEYTARPGARFPVKWTA | P31693 | 6 | DFGLARLIEDNEYTARQGAKFPIKWTA | Q05876 | 6 |
| DFGLARLIEDNEYTARQGAKFPIKWTA | P00523 | 6 | DFGLARLIEDNEYTARQGAKFPIKWTA | Q28923 | 6 |
| DFGLARLIEDNEYTARQGAKFPIKWTA | P00524 | 6 | DFGLARLIEDNEYTARQGAKFPIKWTA | Q9WUD9 | 6 |
| | | | DFGLARVIADDEYCPKQGSRFPVKWTA | P00528 | 6 |